Respiratory Investigation 62 (2024) 901–909

Contents lists available at ScienceDirect

Respiratory Investigation

journal homepage: www.elsevier.com/locate/resinv

Clinical potential of SKP2 as diagnostic marker and therapeutic target in small cell lung cancer

Naohisa Matsumoto [a,b], Ken Tajima [a,b,*], Fumiyuki Takahashi [a,b], Yoichiro Mitsuishi [a,b], Aditya Wirawan [a,b], Moulid Hidayat [a,b], Wira Winardi [a,b], Adityo Wibowo [a,b], Daisuke Hayakawa [a,b], Kenta Izumi [a,b], Koichiro Kanamori [a,b], Yosuke Miyashita [a,b], Takafumi Handa [c], Tetsuhiko Asao [a,b], Ryo Ko [a,b], Takehito Shukuya [a,b], Naoko Shimada [a,b], Kazuya Takamochi [d], Takuo Hayashi [c], Kenji Suzuki [d], Kazuhisa Takahashi [a,b]

[a] Department of Respiratory Medicine, Juntendo University, Graduate School of Medicine, 2-1-1 Hongo, Bunkyo-Ku, Tokyo 113-8421, Japan
[b] Research Institute for Diseases of Old Ages, Juntendo University, Graduate School of Medicine, 2-1-1 Hongo, Bunkyo-Ku, Tokyo 113-8421, Japan
[c] Department of Human Pathology, Juntendo University, Graduate School of Medicine, 2-1-1 Hongo, Bunkyo-Ku, Tokyo 113-8421, Japan
[d] Department of General Thoracic Surgery, Juntendo University, Graduate School of Medicine, 2-1-1 Hongo, Bunkyo-Ku, Tokyo 113-8421, Japan

ARTICLE INFO

Keywords:
SKP2
Small cell lung cancer
Apoptosis
Senescence
Diagnostic marker

ABSTRACT

Background: Small cell lung cancer (SCLC) is the most aggressive type of lung cancer. The overall survival has not improved significantly over the last decades because no major therapeutic breakthroughs have been achieved for over 15 years.
Methods: We analyzed a genome-wide loss-of-function screening database to identify vulnerabilities in SCLC for the development of urgently needed novel therapies.
Results: We identified *SKP2* (encoding S-phase kinase-associated protein 2) and *CKS1B* (encoding CDC28 protein kinase regulatory subunit 1B) as the two most essential genes in that order in SCLC. Notably, SKP2 and CKS1B comprise the p27 binding pocket of the E3 ubiquitin ligase SCF^{SKP2} complex. Immunohistochemistry on tissue microarrays revealed that SKP2 was expressed in >95% of samples at substantially higher levels than that observed for commonly used neuroendocrine markers. As expected, SCLC cell lines were sensitive to SKP2 inhibition. Furthermore, SKP2 or CKS1B knockdown induced apoptosis in *RB1* mutant cells, whereas it induced senescence in *RB1* wild-type cells.
Conclusion: Although the mechanism underlying SKP2 knockdown-induced growth inhibition differs between *RB1*-wild-type and -mutant SCLC, SKP2 can be considered a novel therapeutic target for patients with SCLC regardless of the *RB1* mutation status. Our findings indicate that SKP2 is a potential novel clinical diagnostic marker and therapeutic target in SCLC.

1. Introduction

Small cell lung cancer (SCLC) accounts for approximately 15% of lung cancers and is characterized by poor prognosis [1,2]. Current therapeutic options for SCLC are limited. The standard treatment has been immune-checkpoint inhibitor with or without platinum doublet [3–6]. However, a better understanding of the molecular mechanisms underlying SCLC initiation and progression is warranted to identify novel therapeutic targets for developing more effective chemotherapies.

Whole-genome approaches have identified genetic alterations that have provided new insights into the molecular events in NSCLC, leading to identifying genetic alterations and activated signaling pathways as

Abbreviations: CCLE, Cancer Cell Line Encyclopedia; CKS1B, CDC28 protein kinase regulatory subunit 1B; GO, Gene Ontology; IC_{50}, half-maximal inhibitory concentration; IHC, immunohistochemistry; INSM1, insulinoma-associated protein 1; NSCLC, non-small cell lung cancer; RNAi, RNA interference; RT-qPCR, quantitative reverse transcription PCR; SCF, Skp1-Cullin 1-F-box; SCLC, small cell lung cancer; shRNA, short hairpin RNA; SKP2, S-phase kinase-associated protein 2; TMA, tissue microarray.

* Corresponding author. Department of Respiratory Medicine, Juntendo University, Graduate School of Medicine, 2-1-1 Hongo, Bunkyo-Ku, Tokyo 113-8421, Japan.
E-mail address: tajiken@juntendo.ac.jp (K. Tajima).

https://doi.org/10.1016/j.resinv.2024.07.014
Received 17 January 2024; Received in revised form 27 June 2024; Accepted 22 July 2024
Available online 7 August 2024

potential chemotherapeutic targets [7–10]. A large-scale molecular study in SCLC did not reveal any targetable driver mutations; however, genetic alterations in tumor suppressor genes such as *TP53* and *RB1* that are not yet targetable were frequently observed [11], warranting a novel approach for target identification. Genome-wide loss-of-function screening is an effective approach to identify cancer vulnerabilities or essential genes involved in cancer development and progression to discover novel therapeutic targets in SCLC.

The F-box protein S-phase kinase-associated protein 2 (SKP2) is one of four subunits of the Skp1-Cullin 1-F-box (SCF) complex, SCF^{SKP2}. SKP2 is the substrate specificity factor of the SCF^{SKP2} E3 ubiquitin ligase that is involved in multiple cellular processes through degradation of ubiquitinated targets [12]. The cell-cycle inhibitor p27, which is a SKP2 substrate, is targeted by SCF^{SKP2} for ubiquitination and degradation [13, 14]. The binding and recognition of p27 as a substrate requires CKS1B, which is an essential accessory protein for SCF^{SKP2} [15]. Other SCF^{SKP2} substrates include p21, p57, E2F1, p130, cyclin D, cyclin E, Smad4, Myc, and FOXO1 that are involved in cell-cycle regulation, cell proliferation, and apoptosis [16]. However, SKP2 is an oncogene that critically regulates essential cellular processes in cancer development and progression. SKP2-knockdown induces apoptosis in RB1-deficient cells, including SCLC cells, by inducing synthetic lethality [17,18]. Therefore, SKP2 is a novel potential therapeutic target.

In this study, we analyzed the online database of Broad Institute genome-wide shRNA screening project, Project Achilles, which is genome-wide loss-of-function screening project aimed at identifying gene-knockdown viability effects (dependencies) with the aim of identifying vulnerabilities in SCLC and obtain potential therapeutic targets.

2. Materials and methods

Additional detailed methods are provided in the Online Data Supplement.

2.1. Cell lines

The following cell lines were used: SCLC: SBC3, SBC5, H69, H82, DMS114, H196, DMS273, H187, H446, and CORL279; NSCLC: A549, H2170, Calu3, PC9, HCC827, H1975, H226 and H460; mesothelioma: H2452, H28, MSTO-211, ACC-MESO-1, ACC-MESO-4, and Y-MESO-14; breast cancer: MCF7; hematopoietic cancer: U937 and THP-1; immortalized human mesothelial cells: Met-5A; and immortalized human bronchial epithelial cells: BEAS-2B.

2.2. RNA interference (RNAi)

Lipofection was performed to transfect the cells with three specific small interfering (si)RNAs targeting SKP2 and a non-specific control. The SKP2 target sequences are provided in the Online Data Supplement.

2.3. Viral infection

Lentiviral short hairpin (sh)RNA constructs were purchased from The RNAi Consortium (Sigma-Aldrich, St. Louis, MO, USA). Lentiviral vectors pHCMV-VSV-G and pCMV ∂8.91 were co-transfected into 293T human embryonic kidney cells by lipofection. After 48 h, the supernatants containing the infective virus were used to directly infect the target cells. After incubation for 24 h in growth medium, the transfected cells were selected using puromycin or G418 and pooled for further experiments. The SKP2 shRNA sequences are provided in the Online Data Supplement.

2.4. Quantitative reverse transcription (RT-q) PCR

The RNeasy Mini Kit (Qiagen, Hilden, Germany), ReverTra cDNA Synthesis Kit (Toyobo, Osaka, Japan), and Fast SYBR Green Master Mix (Applied Biosystems, Foster City, CA, USA) were used to extract RNA, generate cDNA, and perform qPCR, respectively. The SKP2 primer sequences are provided in the Online Data Supplement.

2.5. Western blotting

Cells were lysed in RIPA buffer containing protease and phosphatase inhibitors. The proteins (10 μg/lane) were separated using sodium dodecyl sulfate-polyacrylamide gel electrophoresis followed by immunoblotting. Details of the reagents, antibodies, and methods used for immunoblotting are provided in the Online Data Supplement.

2.6. Immunohistochemistry (IHC)

Tumor samples tissues that were obtained from SCLC patients at Juntendo University Hospital. The study was approved by the Institutional Ethics Committee of Juntendo University School of Medicine with waiver of consent (21-019, June 4, 2021; 18–083, Feb 4, 2021). and all participants gave written informed consent. Tumor tissues were stained with anti-SKP2, anti-synaptophysin, anti-chromogranin, anti-CD56, anti-INSM1, anti-ASCL1, anti-POU2F3, and anti-NEUROD1 antibodies. The relevant details are provided in the Online Data Supplement.

2.7. Chemosensitivity assay

Cytotoxicity was assayed using a WST-8/Cell Counting Kit-8 (Wako, Osaka, Japan) after 72 h of incubation with a SKP2 inhibitor (C1; Millipore, Sigma-Aldrich, Darmstadt, Germany).

2.8. Apoptosis assay

The cells were transfected with shSKP2 or shNT and incubated for five days and stained using the MEBCYTO Apoptosis Kit (Annexin V-FITC Kit, Tokyo, Japan). Apoptosis was assessed using fluorescence-activated cell sorting.

2.9. Public datasets

The gene expression data from the Cancer Cell Line Encyclopedia (CCLE) (https://portals.broadinstitute.org/ccle/data) were analyzed using the Project Achilles v2.20.2 dataset (https://portals.broadinstitute.org/achilles) to identify genes involved in SCLC dependencies with enriched genes having a p-value <0.0005. The enriched gene set was functionally annotated using the Gene Ontology (GO) tool in DAVID [19], and GO terms having a Benjamini–Hochberg-corrected p-value of <0.05 were selected.

2.10. Statistical analysis

Statistical analyses were performed using GraphPad Prism 7.0 (GraphPad Software, La Jolla, CA, USA). Unpaired, two-tailed Student's t-test, and ANOVA were used as appropriate to compare mean values. Statistical significance was set at $p < 0.05$.

3. Results

3.1. Identification of SCLC vulnerabilities

Analyzing the Project Achilles data, we identified 197 genes enriched in SCLC ($p < 0.0005$) (Supplementary Table 1). GO analysis of the enriched genes revealed pathways involved in p27 regulation and E2F1 destruction (Table 1). Notably, *SKP2* and *CKS1B*, which encode components of the E3 ubiquitin ligase complex SCF^{SKP2} and form the p27 binding pocket, were ranked in the top two. Analyzing SKP2 expression in various cell lines to identify potential correlation between SKP2 expression and dependency showed that SKP2 expression was higher in

Table 1
Enrichment analysis of the 197 genes.

Pathway analysis	P-Value	Related Gene
Regulation of p27 pathway	0.000647	S-phase kinase associated protein 2 (SKP2) E2F transcription factor 1 (E2F1)
E2F1 Destruction Pathway	0.008052	CDC28 protein kinase regulatory subunit 1B (CKS1B) Transcription factor Dp-1 (TFDP1)

SCLC cell lines than in NSCLC cell lines in the CCLE (Fig. 1A). However, SKP2 expression and dependency was significantly negatively correlated in SCLC but not in NSCLC, indicating that SKP2 may play an important role in SCLC (Fig. 1B and C). Validating SKP2 expression in SCLC cell lines using qPCR and western blotting showed that SKP2 expression was significantly higher in SCLC cell lines than in non-lung cancer and NSCLC cell lines ($p < 0.001$) (Fig. 1D and E). The protein expression of SKP2 and p27, but not p21, tended to be negatively correlated (Fig. 1F). We also investigated the expression of the SKP2 substrates p21 and p27 (Fig. 1G).

3.2. Immunohistochemistry analysis of SKP2

The results of hematoxylin and eosin staining and IHC analysis of SKP2 in Fig. 2A showed that SKP2-positive staining was distributed in the nucleus, whereas synaptophysin and chromogranin A staining were distributed in the cytoplasm and cytomembrane, respectively.

SKP2 staining was more intense than that of synaptophysin and chromogranin A. IHC analysis of samples from 73 patients with SCLC and large cell neuroendocrine carcinoma and had undergone surgical tumor resection was performed using a tissue microarray (TMA). To compare the sensitivity of SKP2 staining with that of commonly used SCLC markers, staining for SKP2, synaptophysin, chromogranin A, CD56 and insulinoma-associated protein 1 (INSM1) was classified as positive or negative. It was observed that SKP2 and INSM1 showed comparable positivity (Fig. 2B). Notably, SKP2 was positive in 95.8% of samples, and the positive rate for SKP2 was higher than that for the other markers (Table 2). We determined whether SKP could be detected in small tissue specimens by performing SKP2 IHC staining of small biopsy specimens, such as transbronchial lung biopsies (Fig. 2C). Similar to that observed for the surgical specimens, SKP2 and INSM1 had comparable positive

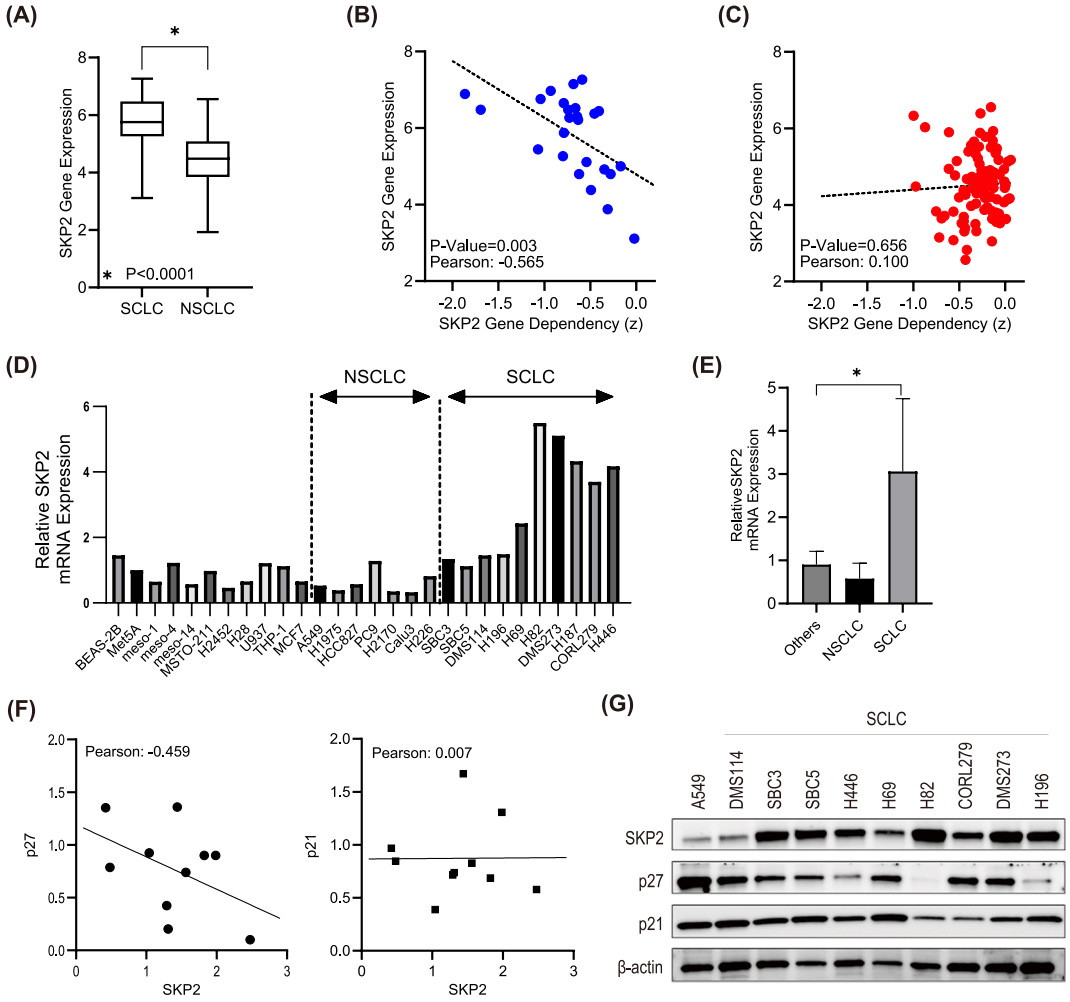

Fig. 1. Identification of small cell lung cancer (SCLC) vulnerabilities
(A) *SKP2* gene expression in SCLC and non-small cell lung cancer (NSCLC) cell lines in the cancer cell line encyclopedia (CCLE) database. *$p < 0.05$, two-tailed unpaired Mann–Whitney test. (B, C) Correlations between SKP2 expression and dependency in SCLC (B) and NSCLC (C) in the CCLE database. Pearson's correlation coefficients are shown. (D) *SKP2* mRNA levels in various cancer cell lines including SCLC (SBC3, SBC5, DMS114, H196, H69, H82, DMS273, H187, CORL279, and H446), NSCLC (A549, H1975, HCC827, PC9, H2170, Calu3, and H226), mesothelioma (ACC-MESO-1, ACC-MESO-4, Y-MESO-14, MSTO-211, H2452, and H28), breast cancer (MCF7), hematopoietic cancer (U937 and THP-1) cells lines, immortalized human mesothelial cells (Met-5A), and immortalized human bronchial epithelial cells (BEAS-2B). (E) Comparison of SKP2 mRNA expression levels in others, NSCLC and SCLC; data are expressed as mean +SD; *$p < 0.05$, two-tailed unpaired Mann–Whitney test. (F) Left: Correlation between SKP2 expression and p27 expression. Right: Correlation between SKP2 expression and p21 expression. Pearson's correlation coefficients are shown. (G) Protein expression of SKP2, p21, and p27. β-actin was the loading control.

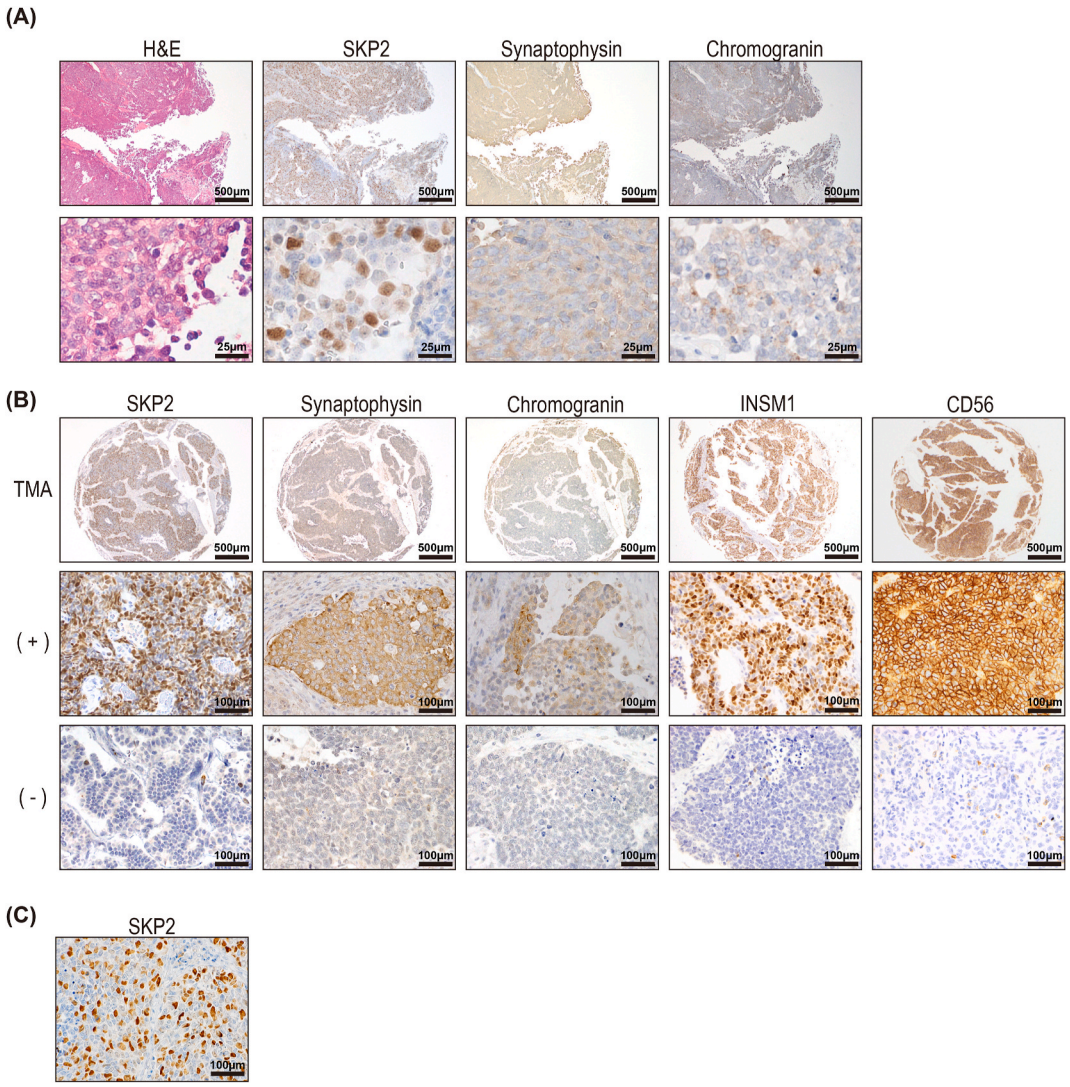

Fig. 2. IHC analysis of SKP2 and neuroendocrine markers in SCLC
(A) Representative hematoxylin and eosin staining and IHC staining of SKP2, synaptophysin, and chromogranin A in SCLC. Upper panel: 4 × magnification. The scale bar represents 500 μm. Lower panel: 80 × magnification. The scale bar represents 25 μm. (B) IHC staining of SKP2, synaptophysin, chromogranin A, CD56, and INSM1 on TMA slides. Representative images of IHC slides to illustrate positive (+) and negative (−) staining of SKP2, chromogranin A, synaptophysin, INSM1, and CD56. Upper panel: 4 × magnification. The scale bar represents 500 μm. Middle and lower panels: 20 × magnification. The scale bar represents 100 μm. (C) IHC staining of SKP2 on small specimens collected used bronchoscopy. 20 × magnification. The scale bar represents 100 μm.

Table 2
Positive SKP2, chromogranin A, synaptophysin, INMS1, and CD56 staining on a tissue microarray (TMA).

N = 73	SKP2	Synaptophysin	Chromogranin A	INSM1	CD56
Positive	70 (95.8%)	66 (90.4%)	29 (39.7%)	62 (84.9%)	58 (79.4%)
Negative	3	7	44	11	15

Table 3
Positive SKP2, INSM1, synaptophysin, chromogranin A, and CD56 expression in immunohistochemistry (IHC) staining of small biopsy specimens.

N = 34	SKP2	INSM1	Synaptophysin	Chromogranin A	CD56
Positive	31 (91.2%)	31 (91.2%)	25 (73.5%)	23 (67.6%)	32 (94.1%)
Negative	3	3	9	11	2

rates but the positive rate for SKP2 was higher than those for other markers, indicating that SKP2 staining can diagnose SCLC (Table 3). To determine the accuracy of SKP2 as a diagnostic marker, we used a TMA consisting of 175 lung adenocarcinoma samples. The positive rate was 18.2% (32/175 cases), which was significantly lower than the positive rate observed in SCLC samples. These results indicated that SKP2 has a high sensitivity (95.8%) and specificity (81.7%) in the diagnosis of SCLC, suggesting that it is a useful discriminative biomarker (Supplementary Table 2). Moreover, in the TMA, all three SKP2-negative cases stained INSM1-positive and all 11 INSM1-negative cases were SKP2-positive (Supplementary Table 3). Similarly, in small biopsy specimens, all three SKP2-negative cases were INSM1-positive and all three INSM1-negative cases were SKP2-positive (Supplementary Table 4). These results suggested an inverse relationship between SKP2 and INSM1. Recently, large transcriptomic data have been used to classify novel molecular subtypes of SCLC [20]; Therefore, additional staining for ASCL1, NEUROD1, and POU2F3 was performed on the SCLC TMA (Supplementary Table 5); however, none of these subtypes showed a correlation with the SKP2 staining results (Supplementary Table 6).

Similarly, we evaluated the subtype expression of cell lines based on literature. The results showed diverse expressions among cell lines, and no bias in subtypes was observed in the cell lines used in our experiments [21].

3.3. SKP2 and CKS1B knockdown induces apoptosis in RB1-mutant cells but not in RB1-wild-type cells

We validate the dependency identified in the Project Achilles data by performing chemosensitivity assays of SCLC and NSCLC cell lines. As expected, the IC_{50} values of the SKP2 inhibitor C1 were significantly lower in SCLC cell lines than in the NSCLC cell lines (Fig. 3A and B). IC_{50} values did not significantly differ between *RB1*-mutant and *RB1*-wild-type SCLC cell lines, indicating that SCLC is sensitive to SKP2 inhibition regardless of the *RB1* mutation status. To address the potential mechanism underlying the high dependency of SCLC on SKP2, we knocked down endogenous SKP2 using lentivirus-driven shRNA constructs (shSKP2) and siRNAs. Two shRNAs (#1 and #2) and three siRNAs (#1, #2, and #3) effectively knocked down endogenous SKP2 protein levels, as confirmed using western blotting (Fig. 3C). Investigating whether SKP2 knockdown induces apoptosis showed that cleaved caspase 3 expression was induced following SKP2 knockdown in *RB1*-mutant SCLC cell lines, H196, and DMS273 but not in DMS114 *RB1*-wild-type SCLC and A549 NSCLC cells (Fig. 3C). Annexin V staining confirmed apoptosis induction in *RB1*-mutant SCLC (Fig. 3D). In addition, we knocked down CSK1B, an essential accessory protein of SCFSKP2 and also ranked in the top two in the Project Achilles data analysis, in *RB1*-mutant/wild-type cell lines. The knockdown efficiencies of siCKS1B and shSKS1B are shown in Supplementary Figs. 1A and B. The results showed that *RB1*-mutant cells were induced into apoptosis, which were the same results as those observed after SKP2 knockdown (Fig. 3E).

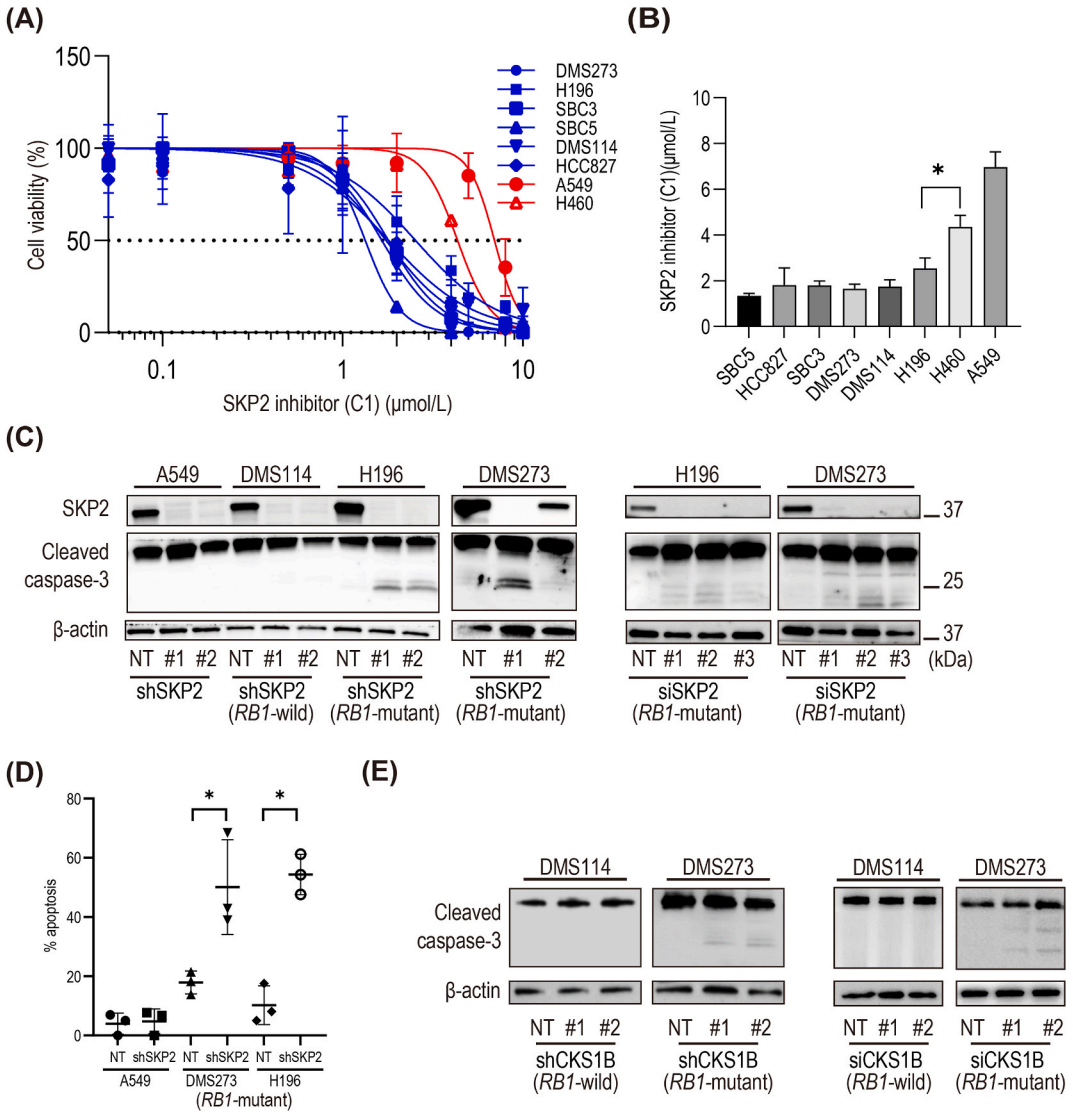

Fig. 3. SKP2 suppression induces apoptosis in *RB1*-mutant cells but not in *RB1*-wild-type cells

(A, B) Chemosensitivity assay in SCLC cell lines and other cancer cell lines in the absence or the presence of the indicated concentrations of the SKP2 inhibitor C1. IC_{50} values are shown in the bar graph. Data from at least three independent experiments are presented as mean +SD. (C) Left: Protein expression of SKP2 and cleaved caspase 3 in A549, DMS114, H196, and DMS273 cells infected with shNT or shSKP2 (#1 and #2). β-actin was the loading control. Right: Protein expression of SKP2 and cleaved caspase 3 in H196 and DMS273 cells transfected with si-control or siSKP2 (#1, #2 and #3). β-actin was the loading control. (D) Percentage of apoptotic cells determined using Annexin V staining. A549, DMS273, and H196 cells transfected with si-control or si SKP2 #1. Data from three independent experiments are presented as mean +SD; *$p < 0.05$, two-tailed unpaired Student's *t*-test. (E) Left: Protein expression of cleaved caspase 3 in DMS114 and DMS273 cells infected with shNT or shCKS1B (#1 and #2). β-actin was the loading control. Right: Protein expression of cleaved caspase 3 in DMS114 and DMS273 cells transfected with si-control or siCKS1B (#1 and #2).

3.4. Mechanism underlying SKP2 knockdown-induced apoptosis in RB1-mutant cells

We investigated the mechanism underlying SKP2 knockdown-induced apoptosis in *RB1*-mutant SCLC by focusing on p27 as C1 prevents p27 from binding to the pocket housing the interface of SKP2 and CSK1B, which were the top two dependencies identified in Project Achilles. Western blotting following SKP2 knockdown showed that p27 protein expression levels increased in both *RB1*-mutant and *RB1*-wild-type cell lines (Fig. 4A). We investigated p27 involvement in SKP2 knockdown-induced apoptosis by generating p27-overexpression *RB1*-mutant cell lines. Unexpectedly, p27 overexpression did not induce cleaved caspase 3 (Fig. 4B), indicating that other molecules are involved in SKP2 knockdown-induced apoptosis. Furthermore, western blotting was performed in *RB1*-mutant cell lines to investigate the expression of the SKP2 substrates c-Myc, FOXO1, CDK2, cyclin D, cyclin E, cyclinA, p27, and p21, which are involved in apoptosis and the cell cycle (Fig. 4C). Cyclin A plays a critical role in SKP2 knockdown-induced synthetic lethality [22]; however, apoptosis showed no correlation with the expression of these proteins.

3.5. SKP2 knockdown induces senescence in RB1-wild-type SCLC

To analyze *RB1*-wild-type SCLC sensitivity to SKP2 knockdown even in the absence of apoptosis induction, we elucidated the mechanisms underlying the high dependency on SKP2 in *RB1*-wild-type SCLC by investigating whether SKP2 knockdown induces senescence as observed previously in cancer cells [23]. As expected, SKP2 knockdown suppressed cell growth in *RB1*-wild-type, DMS114, and SBC3 cells (Fig. 5A). β-Galactosidase staining revealed that β-galactosidase stain-positive *RB1*-wild-type cell numbers increased following SKP2 knockdown, and their morphology was drastically altered with cells presenting a flattened, enlarged, and irregular shape—indicative of SKP2 knockdown-induced senescence (Fig. 5B). The percentage of β-galactosidase stain-positive cells in shSKP2-infected SBC3 and DMS114 cells was significantly higher than that in control cells (Fig. 5C). Thus, SKP2 knockdown induced either apoptosis or senescence depending on the *RB1* mutation status. Interestingly, CKS1B knockdown inhibited cell proliferation and increased the number of β-galactosidase stain-positive cells with a senescent morphology in RB1-wild-type DMS114 and SBC3 cells, indicating that CKS1B knockdown induces senescence in RB1-wild-type SCLC cells (Fig. 5D–F). These results suggested that the SCF^{SKP2} E3 ubiquitin ligase, which is composed of SKP2 and CSK1B, may be a potential therapeutic target for RB1-mutant and wild-type SCLC patients.

4. Discussion

IHC analysis of the neuroendocrine markers effectively improves SCLC diagnosis and its differential diagnosis [24,25]. Synaptophysin and chromogranin A staining are typically weak in SCLC, whereas CD56 is the most sensitive neuroendocrine marker for SCLC. However, 10% of SCLCs are negative for all three commonly used neuroendocrine markers [26–28]. In this study, we demonstrated that SKP2 is highly expressed in SCLC. To our knowledge, this is the first study to compare SKP2 with established SCLC immunostaining markers; SKP2 staining was substantially clearer, intense, and more sensitive than synaptophysin, chromogranin A, and CD56. INSM1 is essential for neuroendocrine differentiation and a recently reported marker for SCLC [29]. In this study, INSM1 and SKP2 showed comparable sensitivity, and as both are nuclear markers, their combined use with conventional cytoplasmic markers may facilitate diagnosis. While the incidence of false negatives for conventional SCLC markers is considerably elevated in limited biopsy specimens, our analysis showed that SKP2 IHC had a sensitivity of 91.2%

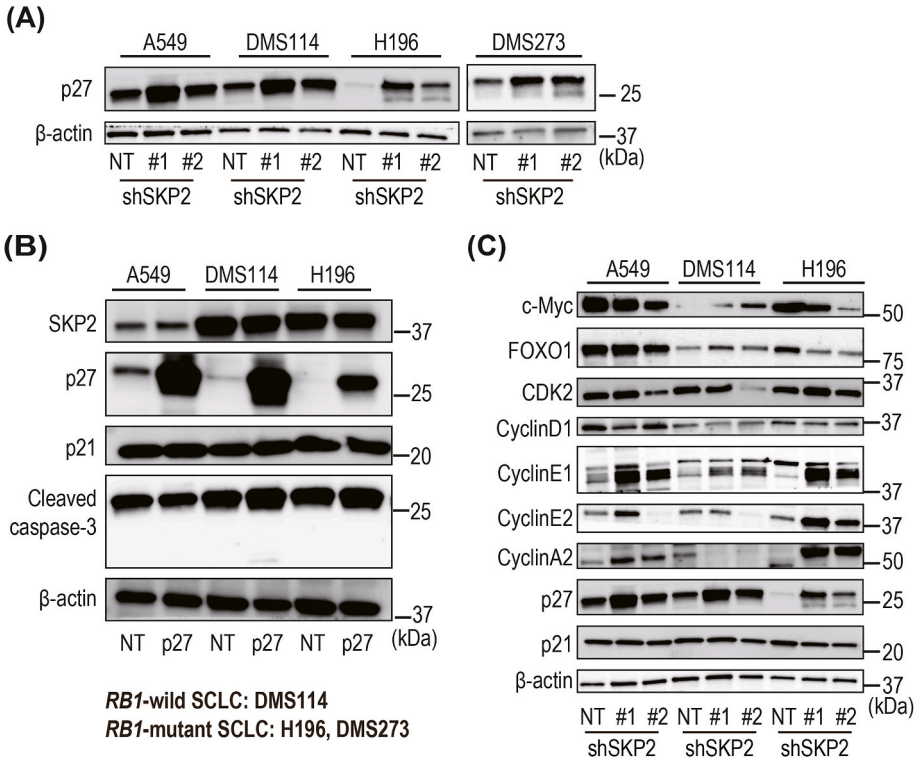

Fig. 4. p27 overexpression fails to induce apoptosis
(A) Protein expression of p27 in A549, DMS114, H196, and DMS273 infected with shNT or shSKP2 (#1 and #2). β-actin was the loading control. (B) Protein expression of SKP2, p27, and cleaved caspase 3 in p27-overexpressing A549, DMS114, and H196 cells. β-actin was the loading control. (C) Protein expression of c-MYC, FOXO1, CDK2, cyclinD1, cyclin E1, cyclin E2, and cyclin A2, p27, p21 in A549, DMS114, and H196 cells infected with shNT or shSKP2 (#1 and #2). β-actin was the loading control.

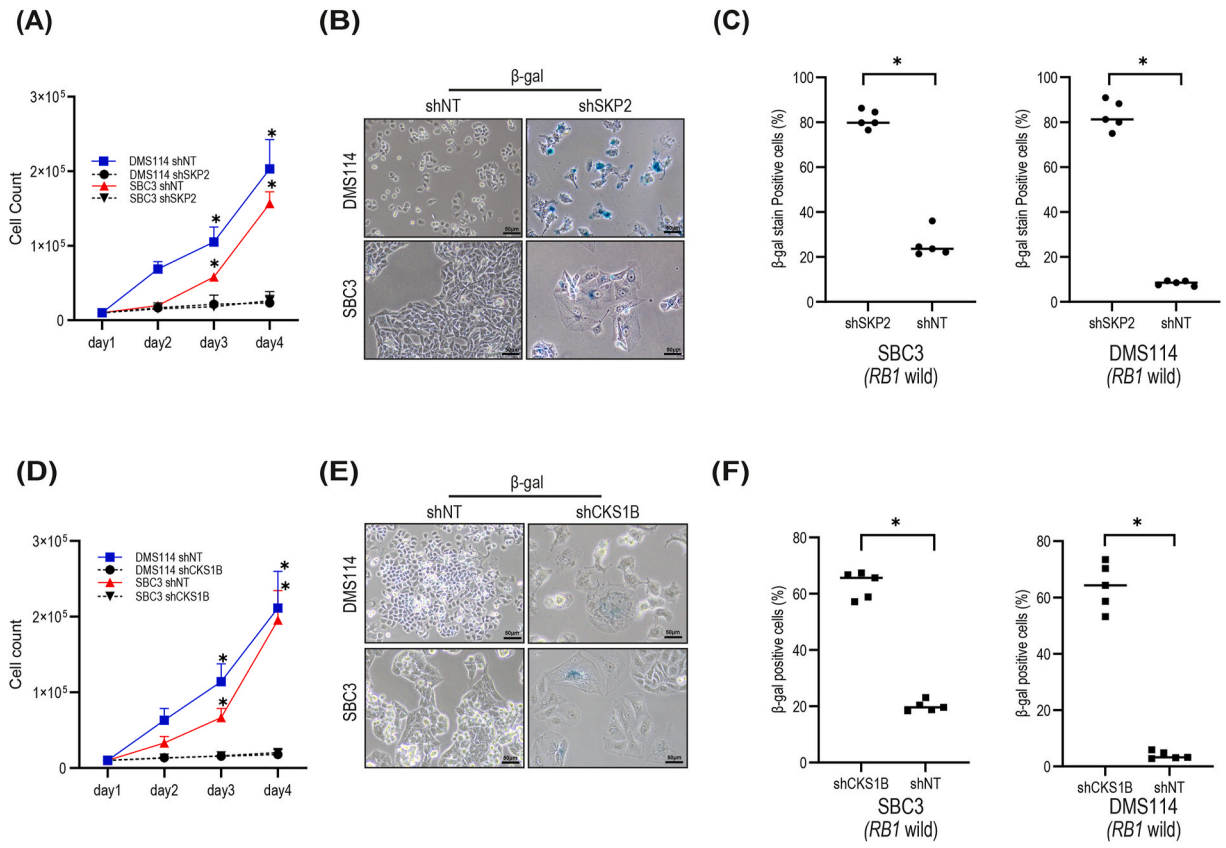

Fig. 5. SKP2 knockdown induces senescence in *RB1*-wild-type SCLC
(A) Proliferation of DMS114 and SBC3 cells infected with shNT or shSKP2. Data from three independent experiments are presented as mean +SD; *$p < 0.05$, two-tailed unpaired Student's *t*-test. (B) β-Galactosidase staining images of DMS114 and SBC3 cells infected with shNT or shSKP2. (C) Quantification of β-galactosidase staining in cells infected with shNT or shSKP2. Data are shown as mean +SD; *$p < 0.05$, two-tailed unpaired Student's *t*-test. (D) Proliferation of DMS114 and SBC3 cells infected with shNT or shCKS1B. Data from three independent experiments are presented as mean +SD; *p < 0.05, two-tailed unpaired Student's t-test. (E) β-Galactosidase staining images of DMS114 and SBC3 cells infected with shNT or shCKS1B. (F) Quantification of β-galactosidase staining in cells infected with shNT or shCKS1B. Data are shown as mean +SD; *p < 0.05, two-tailed unpaired Student's t-.test.

in small biopsies. Notably, SKP2 staining demonstrated superior sensitivity to synaptophysin, chromogranin A, and CD56 staining, and comparable sensitivity to INSM1 staining. Furthermore, all SKP2-negative cases were INSM1-positive and all INSM1-negative cases were-SKP2 positive in both the TMA and small biopsies. In contrast, conventional neuroendocrine markers did not show a relationship with SKP2 or INSM1. This indicates a complementary marker relationship between SKP2 and INSM1, and the combination of SKP2 and INSM1 is expected to further improve diagnostic sensitivity.

SCLCs appear to be converging on a new model of SCLC subtypes defined by differential expression of several transcription factors [30]. Classification into these subtypes reportedly predicts the efficacy of immune checkpoint inhibition [20]. Our TMA analysis showed that SKP2 was present in 95.3% of cases, suggesting its widespread and subtype-independent expression. Consequently, we did not find any potential correlations between these subtypes and SKP2, possibly because of the extremely high positivity rate of SKP2, which allows targeting all subtypes.

TP53 and *RB1* are the most frequently genetically altered SCLC tumor suppressor genes [11]. The primary challenge in targeting tumor suppressor genes is the difficulty in restoring their function, which is overcome by using synthetic lethality [31]. Zhao et al. showed that SKP2 knockdown induced robust apoptosis in RB1-deficient cells by inducing synthetic lethality [18] Thus, SKP2 could be a therapeutic target for patients with RB1-deficient SCLC.

We confirmed the screening findings using chemosensitivity assays using the SKP2 inhibitor C1, which inhibits p27 binding to the SCF^{SKP2} complex [32,33]. As expected, SCLC cells were sensitive to C1, suggesting that p27 is involved in apoptosis in RB1-deficient cell lines. Moreover. SKP2 deletion sufficiently prevented tumorigenesis in RB1-deficient mice. Moreover, these effects of SKP2 deletion were phenocopied by knock-in of a $p27^{T187A}$ mutant that cannot be ubiquitinated by SKP2 [22], indicating that the antitumor effect induced by SKP2 deletion in RB1-deficient mice depends on p27. However, p27 overexpression failed to induce apoptosis in *RB1*-mutant SCLC cell lines. Furthermore, although p27-dependent induction of apoptosis via cyclin A in RB1-deficient cells has been shown [22], cyclin A showed no consistent expression trend and was not involved in the mechanism of action of SKP2. Further studies are required to clarify this.

Next, we investigated the mechanism underlying the high SKP2 dependency in *RB1*-wild-type SCLC. Besides genetic *RB1* alteration, pRb is inactivated by several mechanisms such as p16 loss, cyclin D overexpression, and epigenetic regulation [34,35]. Therefore, the pRb pathway may be inactivated by one of these mechanisms in *RB1*-wild--type SCLC. SKP2 knockdown induced apoptosis in *RB1*-mutant cells but not *RB1*-wild-type cells, indicating that different mechanisms are involved in SKP2 dependency. β-Galactosidase staining results confirmed that SKP2 knockdown induces senescence in *RB1*-wild-type SCLC. Notably, we extended our investigation to CKS1B, a binding partner of SKP2 that forms a complex with SCF^{SKP2}, and found that CKS1B knockdown had similar effects as SKP2 suppression. These results suggest that the SKP2-CKS1B complex plays a critical role in regulating apoptosis or senescence in SCLC cells. Further investigations are required to unravel the mechanism of senescence induced by

suppression of the SKP2-CKS1B complex.

A major limitation of the present study is that the data demonstrating the sensitivity of SCLC cells to SKP2 knockdown were solely obtained from in vitro experiments. Validation of the observed inhibitory effects in an in vivo setting using murine models is warranted. SCLC sensitivity to SKP2 inhibitors resulted in apoptosis in *RB1*-mutant SCLC and senescence in *RB1*-wild-type SCLC. The reasons for the varying outcomes in the presence or absence of *RB1* mutation remain unclear and require further analysis.

5. Conclusions

In conclusion, SKP2 staining is more intense and sensitive than staining for synaptophysin, chromogranin A, or CD56, common neuroendocrine IHC markers of SCLC, and comparable to that of INSM1. There is a complementary relationship between SKP2 and INSM1, suggesting that the combination of SKP2 and INSM1 is expected to further improve diagnostic sensitivity. Both RB1-wild-type and -mutant SCLC cells are sensitive to SKP2 and CKS1B inhibition. Both *RB1*-wild-type and -mutant SCLC cells are sensitive to SKP2 and CKS1B inhibition. Although the detailed underlying mechanisms have not been elucidated, targeting SCF^{SKP2} E3 ubiquitin ligase, which is composed of SKP2 and CSK1B, induced apoptosis in RB1-mutant SCLC and senescence in RB1-wild-type SCLC. As SKP2 is critical to SCLC biology, in addition to aiding clinical diagnosis, SKP2 is a promising therapeutic target for patients with SCLC regardless of the *RB1* mutation status.

Author contributions

NM and KT were central in writing the paper, conceptualizing, and performing and analyzing experiments. FT, TA, YM, TH, and KS contributed to the conception and analysis. AW, MH, WW, AW, DH, KI, KK, YM, TH, and RK were instrumental in performing and analyzing experiments. TS, NS, and KT provided significant contributions to the conception of the work.

All authors have approved the submitted version of the manuscript and agreed to be accountable for any part of the work.

Funding sources

This work was supported by JSPS KAKENHI Grant Number 16K09586 and 20H03535 (Ken Tajima), a Grant for Cross-disciplinary Collaboration, and a Grant from the Institute for Environmental & Gender-specific Medicine, Juntendo University.

Declaration of competing interest

Ken Tajima received research funding from Novartis. Kazuhisa Takahashi received research funding from Chugai Pharm, MSD, Ono Pharm, and Bristol-Myers Squibb. Additionally, Kazuhisa Takahashi acknowledges donations from Eli Lilly Japan, Teijin Pharm, Chugai Pharm, Nippon Boehringer Ingelheim, Kyorin Pharm, Taiho Pharm, and Sanofi. The other authors have no conflicts of interest.

Acknowledgments

We would like to thank Editage for editing and reviewing this manuscript for English language.

Appendix A. Supplementary data

Supplementary data to this article can be found online at https://doi.org/10.1016/j.resinv.2024.07.014.

References

[1] Semenova EA, Nagel R, Berns A. Origins, genetic landscape, and emerging therapies of small cell lung cancer. Genes Dev 2015;29:1447–62. https://doi.org/10.1101/gad.263145.115.
[2] Byers LA, Rudin CM. Small cell lung cancer: where do we go from here? Cancer 2015;121:664–72. https://doi.org/10.1002/cncr.29098.
[3] Evans WK, Shepherd FA, Feld R, Osoba D, Dang P, Deboer G. VP-16 and cisplatin as first-line therapy for small-cell lung cancer. J Clin Oncol 1985;3:1471–7. https://doi.org/10.1200/jco.1985.3.11.1471.
[4] Noda K, Nishiwaki Y, Kawahara M, Negoro S, Sugiura T, Yokoyama A, et al. Irinotecan plus cisplatin compared with etoposide plus cisplatin for extensive small-cell lung cancer. N Engl J Med 2002;346:85–91. https://doi.org/10.1056/NEJMoa003034.
[5] Horn L, Mansfield AS, Szczęsna A, Havel L, Krzakowski M, Hochmair MJ, et al. First-line atezolizumab plus chemotherapy in extensive-stage small-cell lung cancer. N Engl J Med 2018;379:2220–9. https://doi.org/10.1056/NEJMoa1809064.
[6] Paz-Ares L, Dvorkin M, Chen Y, Reinmuth N, Hotta K, Trukhin D, et al. Durvalumab plus platinum-etoposide versus platinum-etoposide in first-line treatment of extensive-stage small-cell lung cancer (CASPIAN): a randomised, controlled, open-label, phase 3 trial. Lancet 2019;394:1929–39. https://doi.org/10.1016/s0140-6736(19)32222-6.
[7] Mok TS, Wu YL, Thongprasert S, Yang CH, Chu DT, Saijo N, et al. Gefitinib or carboplatin-paclitaxel in pulmonary adenocarcinoma. N Engl J Med 2009;361:947–57. https://doi.org/10.1056/NEJMoa0810699.
[8] Maemondo M, Inoue A, Kobayashi K, Sugawara S, Oizumi S, Isobe H, et al. Gefitinib or chemotherapy for non-small-cell lung cancer with mutated EGFR. N Engl J Med 2010;362:2380–8. https://doi.org/10.1056/NEJMoa0909530.
[9] Kwak EL, Bang YJ, Camidge DR, Shaw AT, Solomon B, Maki RG, et al. Anaplastic lymphoma kinase inhibition in non-small-cell lung cancer. N Engl J Med 2010;363:1693–703. https://doi.org/10.1056/NEJMoa1006448.
[10] Drilon A, Wang L, Hasanovic A, Suehara Y, Lipson D, Stephens P, et al. Response to Cabozantinib in patients with RET fusion-positive lung adenocarcinomas. Cancer Discov 2013;3:630–5. https://doi.org/10.1158/2159-8290.cd-13-0035.
[11] George J, Lim JS, Jang SJ, Cun Y, Ozretić L, Kong G, et al. Comprehensive genomic profiles of small cell lung cancer. Nature 2015;524:47–53. https://doi.org/10.1038/nature14664.
[12] Frescas D, Pagano M. Deregulated proteolysis by the F-box proteins SKP2 and beta-TrCP: tipping the scales of cancer. Nat Rev Cancer 2008;8:438–49. https://doi.org/10.1038/nrc2396.
[13] Nakayama K, Nagahama H, Minamishima YA, Matsumoto M, Nakamichi I, Kitagawa K, et al. Targeted disruption of Skp2 results in accumulation of cyclin E and p27(Kip1), polyploidy and centrosome overduplication. EMBO J 2000;19:2069–81. https://doi.org/10.1093/emboj/19.9.2069.
[14] Nakayama K, Nagahama H, Minamishima YA, Miyake S, Ishida N, Hatakeyama S, et al. Skp2-mediated degradation of p27 regulates progression into mitosis. Dev Cell 2004;6:661–72. https://doi.org/10.1016/s1534-5807(04)00131-5.
[15] Zhan F, Colla S, Wu X, Chen B, Stewart JP, Kuehl WM, et al. CKS1B, overexpressed in aggressive disease, regulates multiple myeloma growth and survival through SKP2- and p27Kip1-dependent and -independent mechanisms. Blood 2007;109:4995–5001. https://doi.org/10.1182/blood-2006-07-038703.
[16] Wang Z, Gao D, Fukushima H, Inuzuka H, Liu P, Wan L, et al. Skp2: a novel potential therapeutic target for prostate cancer. Biochim Biophys Acta 2012;1825:11–7. https://doi.org/10.1016/j.bbcan.2011.09.002.
[17] Brough R, Gulati A, Haider S, Kumar R, Campbell J, Knudsen E, et al. Identification of highly penetrant Rb-related synthetic lethal interactions in triple negative breast cancer. Oncogene 2018;37:5701–18. https://doi.org/10.1038/s41388-018-0368-z.
[18] Zhao H, Iqbal NJ, Sukrithan V, Nicholas C, Xue Y, Yu C, et al. Targeted inhibition of the E3 ligase SCF(Skp2/Cks1) has antitumor activity in RB1-deficient human and mouse small-cell lung cancer. Cancer Res 2020;80:2355–67. https://doi.org/10.1158/0008-5472.can-19-2400.
[19] Dennis Jr G, Sherman BT, Hosack DA, Yang J, Gao W, Lane HC, et al. DAVID: database for annotation, visualization, and integrated discovery. Genome Biol 2003;4:P3.
[20] Gay CM, Stewart CA, Park EM, Diao L, Groves SM, Heeke S, et al. Patterns of transcription factor programs and immune pathway activation define four major subtypes of SCLC with distinct therapeutic vulnerabilities. Cancer Cell 2021;39:346–360 e7. https://doi.org/10.1016/j.ccell.2020.12.014.
[21] Tlemsani C, Pongor L, Elloumi F, Girard L, Huffman KE, Roper N, et al. SCLC-CellMiner: a resource for small cell lung cancer cell line genomics and pharmacology based on genomic signatures. Cell Rep 2020 Oct 20;33(3):108296. https://doi.org/10.1016/j.celrep.2020.108296.
[22] Lu Z, Bauzon F, Fu H, Cui J, Zhao H, Nakayama K, et al. Skp2 suppresses apoptosis in Rb1-deficient tumours by limiting E2F1 activity. Nat Commun 2014;5:3463. https://doi.org/10.1038/ncomms4463.
[23] Tajima K, Matsuda S, Yae T, Drapkin BJ, Morris R, Boukhali M, et al. SETD1A protects from senescence through regulation of the mitotic gene expression program. Nat Commun 2019;10:2854. https://doi.org/10.1038/s41467-019-10786-w.
[24] Travis WD. Update on small cell carcinoma and its differentiation from squamous cell carcinoma and other non-small cell carcinomas. Mod Pathol 2012;25(Suppl 1):S18–30. https://doi.org/10.1038/modpathol.2011.150.
[25] Travis WD. Pathology and diagnosis of neuroendocrine tumors: lung neuroendocrine. Thorac Surg Clin 2014;24:257–66. https://doi.org/10.1016/j.thorsurg.2014.04.001.

[26] Lyda MH, Weiss LM. Immunoreactivity for epithelial and neuroendocrine antibodies are useful in the differential diagnosis of lung carcinomas. Hum Pathol 2000;31:980–7. https://doi.org/10.1053/hupa.2000.9076.
[27] Yesner R. Heterogeneity of so-called neuroendocrine lung tumors. Exp Mol Pathol 2001;70:179–82. https://doi.org/10.1006/exmp.2001.2373.
[28] Zheng G, Ettinger DS, Maleki Z. Utility of the quantitative Ki-67 proliferation index and CD56 together in the cytologic diagnosis of small cell lung carcinoma and other lung neuroendocrine tumors. Acta Cytol 2013;57:281–90. https://doi.org/10.1159/000346394.
[29] Mukhopadhyay S, Dermawan JK, Lanigan CP, Farver CF. Insulinoma-associated protein 1 (INSM1) is a sensitive and highly specific marker of neuroendocrine differentiation in primary lung neoplasms: an immunohistochemical study of 345 cases, including 292 whole-tissue sections. Mod Pathol 2019;32:100–9. https://doi.org/10.1038/s41379-018-0122-7.
[30] Rudin CM, Poirier JT, Byers LA, Dive C, Dowlati A, George J, et al. Molecular subtypes of small cell lung cancer: a synthesis of human and mouse model data. Nat Rev Cancer 2019;19:289–97. https://doi.org/10.1038/s41568-019-0133-9.
[31] Nijman SM. Synthetic lethality: general principles, utility and detection using genetic screens in human cells. FEBS Lett 2011;585:1–6. https://doi.org/10.1016/j.febslet.2010.11.024.
[32] Rico-Bautista E, Wolf DA. Skipping cancer: small molecule inhibitors of SKP2-mediated p27 degradation. Chem Biol 2012;19:1497–8. https://doi.org/10.1016/j.chembiol.2012.12.001.
[33] Wu L, Grigoryan AV, Li Y, Hao B, Pagano M, Cardozo TJ. Specific small molecule inhibitors of Skp2-mediated p27 degradation. Chem Biol 2012;19:1515–24. https://doi.org/10.1016/j.chembiol.2012.09.015.
[34] De La Rosa-Velázquez IA, Rincón-Arano H, Benítez-Bribiesca L, Recillas-Targa F. Epigenetic regulation of the human retinoblastoma tumor suppressor gene promoter by CTCF. Cancer Res 2007;67:2577–85. https://doi.org/10.1158/0008-5472.can-06-2024.
[35] Gordon GM, Du W. Targeting Rb inactivation in cancers by synthetic lethality. Am J Cancer Res 2011;1:773–86.